Modeling and characterization of metal-semiconductor-metal-based source-drain contacts in amorphous InGaZnO thin film transistors

Sangwon Lee,[1] Jun-Hyun Park,[1] Kichan Jeon,[1] Sungchul Kim,[1] Yongwoo Jeon,[1] Dae Hwan Kim,[1] Dong Myong Kim,[1,a)] Jae Chul Park,[2] and Chang Jung Kim[2]
[1]*School of Electrical Engineering, Kookmin University, 861-1 Jeongneung-dong, Seongbuk-gu, Seoul 136-702, Republic of Korea*
[2]*Semiconductor Laboratory, Samsung Advanced Institute of Technology, Nongseo-Dong, Giheung-Gu, Yongin-Si, Gyeonggi-Do 446-712, Republic of Korea*

(Received 4 January 2010; accepted 23 February 2010; published online 15 March 2010)

Due to the inherent property of large contact and parasitic resistances in amorphous InGaZnO (*a*-IGZO) thin film transistors (TFTs), a metal-semiconductor-metal (MSM) structure is a key element in *a*-IGZO TFTs. Therefore, voltage drops across resistances and MSM structure should be fully considered in the modeling and characterization of *a*-IGZO TFTs. A physics-based semiempirical model for the current-voltage characteristics of the MSM structure for the source-channel-drain contact in *a*-IGZO TFTs is proposed and verified with experimental results. The proposed model for the current in *a*-IGZO MSM structures includes a thermionic field emission $[J_{\mathrm{TFE}} \propto \exp(V_{R,\mathrm{Schottky}}/V_o)]$ and trap-assisted generation $(J_{\mathrm{gen}} \propto \sqrt{V_{R,\mathrm{Schottky}}})$ in addition to the thermionic emission current (J_S: Independent of the bias) under reverse bias. Experimental result suggests that electrical characteristics of the MSM structure depend not only on the Schottky barrier but also on the bulk property of the *a*-IGZO active layer. © *2010 American Institute of Physics*. [doi:10.1063/1.3364134]

Amorphous oxide thin film transistors (TFTs) are expected to be widely employed as switching devices for active-matrix liquid crystal displays/active-matrix organic light-emitting diodes because of the advantages in large scale integration, low cost room temperature (RT) fabrication process, high mobility, and compatibility with transparent and electronic paper applications.[1,2] Characterization of the contact property between the source/drain (S/D) metal and the amorphous InGaZnO (*a*-IGZO) semiconductor active layer is important because a high series resistance in the S/D contacts causes degradation of electrical performance in threshold voltage (V_T), field effect mobility (μ_{FE}), $I_{\mathrm{on}}/I_{\mathrm{off}}$ ratio, subthreshold swing (SS), and other short channel effect.[3] Due to large parasitic resistances inherent in *a*-IGZO TFTs, voltage drops across resistances should be considered in the modeling and characterization with the transfer length.[3] For circuit applications of *a*-IGZO TFTs, physical mechanisms for the current transport should be considered in the modeling and characterization of the metal-semiconductor-metal (MSM) structure. In this work, a physics-based semiempirical model for the current transport in the MSM structure for S/D contacts is proposed and their modeling parameters are characterized for robust design and assessment of *a*-IGZO TFTs and their integrated circuits.

Fabricated TFTs have an inverted staggered bottom gate (thickness of SiO_2: $T_{GI}=100$ nm) with *a*-IGZO active layer ($T_{\mathrm{IGZO}}=70$ nm) deposited by rf magnetron sputtering at RT. The channel length (L), the width (W), and the overlap (L_{ov}) between the gate and S/D are designed to be $L=2$ μm, $W=200$ μm, and $L_{ov}=10$ μm, respectively. A schematic cross-section of the integrated *a*-IGZO TFTs is shown in the inset of Fig. 1(a) by the process sequence described in Ref. 4. Both the transfer and output characteristics of the fabricated *a*-IGZO TFT are shown in Figs. 1(a) and 1(b), respectively. Characteristic parameters are obtained to be $V_T=-0.75$ V, $\mu_{FE}=11.4$ cm^2/Vs, and $SS=370$ mV/dec.

a-IGZO TFTs contain an MSM structure between the source-semiconducting *a*-IGZO active layer-drain due to the contact formation process on the semiconducting wide band gap *a*-IGZO layer ($E_g>3.0$ eV). It can be electrically modeled as a series connection of two Schottky diodes with a resistor between them as shown in the inset of Fig. 2(a). The energy band diagram for the conduction mechanism in the MSM structure is schematically shown in Fig. 2(b) as an inset. In the S/D MSM structure, we obtain

$$I_{DS} = I_{R,\mathrm{Schottky}} = I_{\mathrm{IGZO}} = I_{F,\mathrm{Schottky}}, \tag{1}$$

$$V_{DS} = V_{R,\mathrm{Schottky}} + V_R + V_{\mathrm{IGZO}} + V_{F,\mathrm{Schottky}} \approx V_{R,\mathrm{Schottky}} + V_{\mathrm{IGZO}} + V_{F,\mathrm{Schottky}}, \tag{2}$$

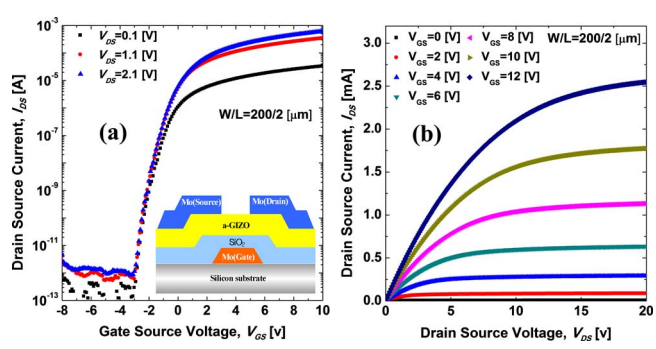

FIG. 1. (Color online) (a) Measured transfer (I_{DS}-V_{GS}) characteristics with a schematic structure as an inset and (b) output (I_{DS}-V_{DS}) characteristics of the fabricated *a*-IGZO TFT with W/L=200 μm/2 μm.

a)Electronic mail: dmkim@kookmin.ac.kr.

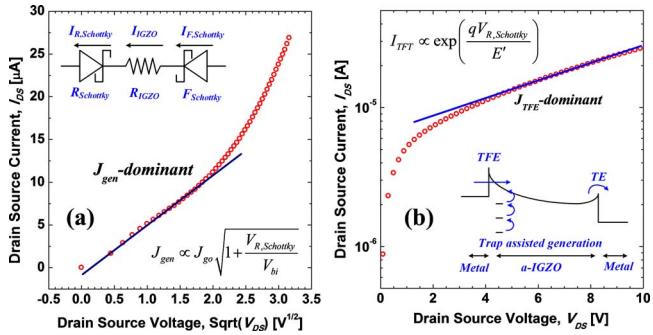

FIG. 2. (Color online) Measured current voltage characteristics of the MSM structure. (a) I_{DS}-$\sqrt{V_{DS}}$ curve for characterization of the J_{gen}-dominant operation with an equivalent circuit as an inset and (b) I_{DS}-V_{DS} curve for charactering the J_{TFE}-dominant region with a schematic energy band diagram for current mechanisms as an inset.

$$V_{R,\text{Schottky}} + V_{F,\text{Schottky}} \cong V_{R,\text{Schottky}}, \tag{3}$$

with $I_{DS}(V_{DS})$: the drain current(voltage) across the MSM structure, $I_{\text{IGZO}}(V_{\text{IGZO}})$: Current (voltage) through the *a*-IGZO active layer, $I_{R,\text{Schottky}}(V_{R,\text{Schottky}})$ and $I_{R,\text{Schottky}}(V_{R,\text{Schottky}})$: Current (voltage) across the reverse- and forward-biased Schottky diodes, and V_R: Voltage drop across the S/D parasitic resistance. Current in the MSM structure for the S/D contact is limited by the reverse biased Schottky contact and there are mainly three current components; (i) thermal generation current (J_{gen}), (ii) thermionic field emission current (J_{TFE}), and (iii) thermionic emission current (J_S) in the reverse biased Schottky diode (Ref. 5). Investigating the bias-dependence of the current in the experimental data, the trap-assisted generation current (J_{gen}) (Ref. 6) in the space charge region (SCR) is observed to be the main component under a low drain bias [Fig. 2(a)]. Although the band gap energy of the *a*-IGZO layer is very high (~3 eV), trapped electrons under the Fermi level (E_F) in the *a*-IGZO channel layer can be thermally excited through the subgap energy states distributed over the band gap. On the other hand, the thermionic field emission current (J_{TFE}) (Ref. 7) is dominant under a large reverse bias [Fig. 2(b)].

The trap-assisted thermal generation current J_{gen} through traps in the SCR is described by

$$J_{\text{gen}} = q\int_0^X g_{th}dx = J_{go}\sqrt{\left(1+\frac{V_{R,\text{Schottky}}}{V_{bi}}\right)} \times\left[1-\exp\left(-\frac{V_{R,\text{Schottky}}}{V_{th}}\right)\right] \ [\text{A/cm}^2], \tag{4}$$

$$J_{go} \equiv \frac{qn_i}{2\tau_o}\sqrt{\frac{2\varepsilon_{\text{IGZO}}V_{bi}}{qN_D}} \ [\text{A/cm}^2], \tag{5}$$

where n_i, τ_o, $\varepsilon_{\text{IGZO}}$, N_D, and V_{bi} are the intrinsic carrier density, lifetime, permittivity, donor density in the *a*-IGZO active layer, and the built-in voltage in the Schottky contact, respectively. We note that J_{gen} is proportional to $\sqrt{(1+V_{R,\text{Schottky}}/V_{bi})}$ and the characteristic current density J_{go} is determined by the bulk property of the *a*-IGZO layer.

The thermionic field emission current J_{TFE}, formed by thermal excitation of electrons and continuous tunneling through the Schottky barrier from the metal to the *a*-IGZO channel layer under large reverse bias and, is described by

$$J_{\text{TFE}} = J_{\text{TFEo}}\exp\left(+\frac{qV_{R,\text{Schottky}}}{E'}\right), \tag{6}$$

$$J_{\text{TFEo}} = \frac{A^*T^2\sqrt{\pi E_{00}}}{kT}\sqrt{qV_R+\frac{E_B}{\cosh(E_{00}/kT)}}\exp\left(-\frac{E_B}{E_0}\right), \tag{7}$$

$$E' = E_{00}\left[\frac{E_{00}}{kT}-\tanh\left(\frac{E_{00}}{kT}\right)\right],$$

$$E_0 = E_{00}\coth(E_{00}/kT), \quad E_{00} = \frac{\hbar}{2}\sqrt{\frac{N_D}{m^*_{\text{IGZO}}\varepsilon_{\text{IGZO}}}}, \tag{8}$$

where A^*, T, E_B, $\hbar$, and m^*_{IGZO} are the Richardson constant, temperature, Schottky barrier, the Plank constant, and the effective mass of electrons in the *a*-IGZO layer, respectively. E', E_0, and E_{00} are characteristic energies for the thermionic field emission current.[7] We also note that J_{TFE} is proportional to $\exp(qV_{R,\text{Schottky}}/E')$.

The thermionic emission current J_S is formed by electrons overcoming the Schottky barrier by the thermal energy from the metal to the *a*-IGZO channel layer. It is described by $J_S = A^*T^2\exp(-E_B/kT)$ and independent of the reverse bias. Therefore, the dominant mechanisms across the MSM structure are expected to be the trap-assisted generation current J_{gen} and the thermionic field emission current J_{TFE} under reverse bias as described by

$$J_{R,\text{Schottky}} = J_{\text{gen}} + J_{\text{TFE}} + J_S. \tag{9}$$

The property of contacts on the *a*-IGZO layer depends not only on the Schottky barrier E_B but also on the bulk property of the *a*-IGZO channel layer. Therefore, it is strongly subject to the fabrication process such as rf power, O_2 partial pressure, and thickness of the *a*-IGZO active layer.[8–10]

Due to the inherent property of *a*-IGZO TFTs, the voltage drop across large channel and parasitic resistances should be considered in the modeling and characterization of the MSM structure. The total resistance is composed of the external load resistance (R_L), source resistance (R_S), drain resistance (R_D), and V_{GS}-dependent channel resistance (R_{ch}). The contact resistance ($R_C = R_S + R_D$) can be extracted by using the modified external loading method[11] connecting an external load resistor to the source terminal. Considering the voltage drop on resistances, the drain current I_{DS} in TFTs under linear operation is described by

$$I_{DS} = K\{V_{GS} - I_{DS}(R_S+R_L) - V_T - 0.5[V_{DS} - I_{DS}(R_S+R_D+R_L)]\} \times [V_{DS} - I_{DS}(R_S+R_D+R_L)], \tag{10}$$

where $K = \mu C_{ox}(\text{W/L})$ with μ=the channel carrier mobility and C_{ox}=the effective gate capacitance per unit area (F/cm^2). Under linear mode of operation with a small drain bias V_{DS}, we obtain

$$\frac{1}{I_{DS}} = \frac{R_L+R_S+R_D}{V_{DS}} + \frac{1}{K(V_{GS}-V_T-0.5V_{DS})V_{DS}}. \tag{11}$$

By plotting $1/I_{DS}$ versus R_L as a function of V_{GS}, R_{Lo} from the intercept in Fig. 3(a) can be obtained to be

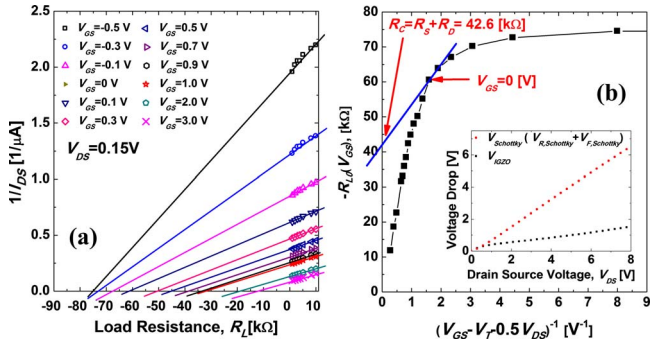

FIG. 3. (Color online) Extraction of the S/D contact resistance $R_C=R_S+R_D$ through the external load resistance method (Ref. 11). (a) $1/I_{DS}$ vs external load resistance R_L as a function of V_{GS} and (b) $-R_{L0}$ vs $1/(V_{GS}-V_T-0.5V_{DS})^{-1}$ curve to get $R_C=R_S+R_D$. The inset shows voltage drops in the channel and contact region calculated from the extracted resistance from experimental data.

$$-R_{Lo}(V_{GS}) = R_S + R_D + \frac{1}{K(V_{GS} - V_T - 0.5V_{DS})}. \qquad (12)$$

By plotting the V_{GS}-dependent $-R_{Lo}$ as a function of $1/(V_{GS}-V_T-0.5V_{DS})$, $R_C=R_S+R_D$ can be extracted as shown in the Fig. 3(b). In the linear mode (V_{DS}=0.15 V), the total resistances from two I_{DS}-V_{DS} curves are extracted to be almost the same as $R_{T,\text{gate\_floating}}$=121 kΩ when the gate electrode is floated and $R_{T,VGS=0\ V}$=132 kΩ at V_{GS}=0 V. Since we modeled that $R_C=R_S+R_D$ is independent of V_{GS}, the difference in the total resistance is caused by the V_{GS}-dependent channel resistance. With V_{GS}-dependent channel resistance, the S/D contact resistance is extracted to be R_C=42.6 kΩ. Each voltage drop in the channel and contact region is calculated considering the extracted resistance from experimental data shown in Fig. 3(b) as an inset.

Extraction of model parameters using the physics-based model for the MSM structure in the *a*-GIZO TFT is shown in Fig. 4(a). The Schottky barrier, denoted in the inset of Fig. 4(a), of the contact from the thermionic emission current component J_{TFEo} is obtained to be E_B=0.216 eV. By plotting $\sqrt{(1+V_{R,\text{Schottky}}/V_{bi})}$ versus I_D in the J_{gen}-dominant region, V_{bi} can be obtained from the intersection in Fig. 4(a). On the other hand, by plotting $V_{R,\text{Schottky}}$ versus $\log(I_D)$ in the J_{TFE}-dominant region where J_{TFE} is proportional to $\exp(qV_{R,\text{Schottky}}/E')$, N_D is extracted from the slope in Fig. 4(a). In Fig. 4(b) for V_{GS}=0 V, I_{DS}-V_{DS} characteristics of the *a*-IGZO MSM structure are compared with the physics-based semiempirical model for the effective contact area A_{eff}=100 μm^2 considering the channel width and the transfer length of the metal contact.[3] Experimental I-V curve agrees well with the physics-based semiempirical model adopting experimentally extracted model parameters (J_{go}=526.7 A/cm^2, τ_o=2.73 μs, $\varepsilon_{\text{IGZO}}$=11.5 ε_o, N_D=1.01 × x 10^{17} cm^{-3}, m^*_{IGZO}=0.15m_o, and V_{bi}=0.097 V).

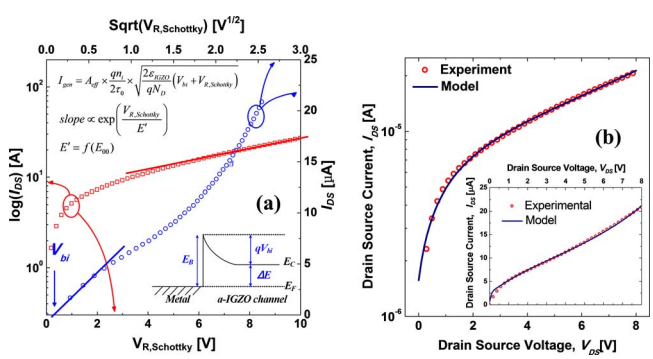

FIG. 4. (Color online) Extraction of model parameters and verification of the physics-based model for the MSM structure in *a*-GIZO TFTs. (a) Extraction of physics-based model parameters from experimental data (E_B=0.216 eV, N_D=1.01× x 10^{17} cm^{-3}, V_{bi}=0.097 V). (b) Measured I_{DS}-V_{DS} characteristics of the *a*-IGZO MSM structure are compared with the physics based semiempirical model for V_{GS}=0 V.

In conclusion, voltage drops across resistances should be considered in the modeling and characterization because *a*-IGZO TFTs contain an MSM structure due to inherent property of large contact and parasitic S/D resistances. A physics based semiempirical model for the current-voltage characteristics of the source-channel-drain MSM contact in *a*-IGZO TFTs was proposed, model parameters are extracted, and verified by comparison of the experimental data. In the model for *a*-IGZO MSM structures, a thermionic field emission and trap-assisted generation were considered in addition to the thermionic emission current under reverse bias. Experimental result suggests that contact characteristics are strongly dependent not only on the Schottky barrier but also on the bulk property of the *a*-IGZO active layer.

This work was supported by the National Research Foundation of Korea (NRF) grant funded by the Korea government (MEST) (Grant No. 2009–0080344). The CAD software was supported by SILVACO and IC Design Education Center (IDEC).

[1] J. K. Jeong, J. H. Jeong, J. H. Choi, J. S. Im, S. H. Kim, H. W. Yang, K. N. Kang, K. S. Kim, T. K. Ahn, H.-J. Chung, M. Kim, B. S. Gu, J.-S. Park, Y.-G. Mo, H. D. Kim, and H. K. Chung, SID Int. Symp. Digest Tech. Papers **39**, 1 (2008).
[2] J.-H. Lee, D.-H. Kim, D.-J. Yang, S.-Y. Hong, K.-S. Yoon, P.-S. Hong, C.-O. Jeong, H.-S. Park, S. Y. Kim, S. K. Lim, S. S. Kim, K.-S. Son, T.-S. Kim, J.-Y. Kwon, and S.-Y. Lee, SID Int. Symp. Digest Tech. Papers **39**, 625 (2008).
[3] J. Park, C. Kim, S. Kim, I. Song, S. Kim, D. Kang, H. Lim, H. Yin, R. Jung, E. Lee, J. Lee, K.-W. Kwon, and Y. Park, IEEE Electron Device Lett. **29**, 879 (2008).
[4] K. Jeon, C. Kim, I. Song, J. Park, S. Kim, S. Kim, Y. Park, J.-H. Park, S. Lee, D. M. Kim, and D. H. Kim, Appl. Phys. Lett. **93**, 182102 (2008).
[5] E. H. Rhoderick, *Metal-Semiconductor Contact* (Oxford Science, New York, 1980).
[6] S. W. Kim, K. S. Roh, S. H. Seo, K. Y. Kim, G. C. Kang, S. Lee, C. M. Choi, S. R. Park, J. H. Park, K. C. Chun, K. J. Song, D. H. Kim, and D. M. Kim, Microelectron. Reliab. **48**, 382 (2008).
[7] S. M. Sze, *Physics of Semiconductor Devices*, 2nd ed. (Wiley, New York, 1981).
[8] Y. Orikasa, N. Hayashi, and S. Muranaka, J. Appl. Phys. **103**, 113703 (2008).
[9] K. Nomura, H. Ohta, A. Takagi, T. Kamiya, M. Hirano, and H. Hosono, Nature (London) **432**, 488 (2004).
[10] A. Suresh, P. Wellenius, A. Dhawan, and J. Muth, Appl. Phys. Lett. **90**, 123512 (2007).
[11] B.-Y. Tsui, C.-P. Lu, and H.-H. Liu, IEEE Electron Device Lett. **29**, 1053 (2008).